JACS
JOURNAL OF THE AMERICAN CHEMICAL SOCIETY

ARTICLE

pubs.acs.org/JACS

pH-Induced Intramolecular Folding Dynamics of i-Motif DNA

Jungkweon Choi, Sooyeon Kim, Takashi Tachikawa, Mamoru Fujitsuka, and Tetsuro Majima*

The Institute of Scientific and Industrial (SANKEN), Osaka University, Mihogaoka 8-1, Ibaraki, Osaka 567-0047 Japan

Supporting Information

ABSTRACT: Using the combination of fluorescence resonance energy transfer (FRET) and fluorescence correlation spectroscopy (FCS) technique, we investigate the mechanism and dynamics of the pH-induced conformational change of i-motif DNA in the bulk phases and at the single-molecule level. Despite numerous studies on i-motif that is formed from cytosine (C)-rich strand at slightly acidic pH, its detailed conformational dynamics have been rarely reported. Using the FRET technique to provide valuable information on the structure of biomolecules such as a protein and DNA, we clearly show that the partially folded species as well as the single-stranded structure coexist at neutral pH, supporting that the partially folded species may exist substantially in vivo and play an important role in a process of gene expression. By measuring the FCS curves of i-motif, we observed the gradual decrease of the diffusion coefficient of i-motif with increasing pH. The quantitative analysis of FCS curves supports that the gradual decrease of diffusion coefficient (D) associated with the conformational change of i-motif is not only due to the change in the intermolecular interaction between i-motif and solvent accompanied by the increase of pH but also due to the change of the shape of DNA. Furthermore, FCS analysis showed that the intrachain contact formation and dissociation for i-motif are 5−10 times faster than that for the open form. The fast dynamics of i-motif with a compact tetraplex is due to the intrinsic conformational changes at the fluorescent site including the motion of alkyl chain connecting the dye to DNA, whereas the slow intrachain contact formation observed from the open form is due to the DNA motion corresponding to an early stage interaction in the folding process of the unstructured open form.

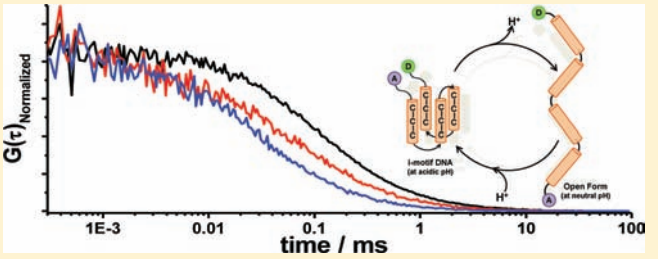

1. INTRODUCTION

DNA, which acts as the carrier of the genetic information, has a right-handed double helical structure under ordinary physiological conditions. In contrast, repetitive DNA sequences under certain conditions may fold into non-B structures, such as hairpin, triplex, cruciform, left-handed Z-form, tetraplex, etc.[1−3] Since these non-B structure-forming sequences induce the genetic instability and consequently may cause human diseases, the molecular mechanism for their genetic instability has been extensively investigated.[1,2] Especially, it is known that tetraplex DNA-forming sequences are observed frequently in the promoter region of oncogene and human telomeric DNA. Thus, tetraplex DNA, such as intermolecular and/or intramolecular G-quadruplex and i-motif structures, have been an emerging topic in nucleic acids research because they can act as a signpost and a controller for the oncogene expression at the transcription level.[4−10] Furthermore, tetraplex DNA with a higher order structure is regarded as a fascinating material for the nanomachine application[11−15] as well as drug delivery system.[16,17] For instance, Shieh et al. reported that G-quadruplex-TMPyP4 (5,10,15,20-tetrakis-(*N*-methyl-pyridnium)-21*H*,23*H*-porphirin) complex destroys cancer cells selectively under 435 nm irradiation. This means that G-quadruplex can be used as a drug carrier for photodynamic therapy for cancer cells.[16] In addition, Modi et al. developed an i-motif-based nanomachine to map the spatial and temporal pH changes associated with endosome maturation.[14] These studies suggest the great potential of DNA scaffolds responsive to complex triggers in sensing, diagnostics, and targeted therapies in a living cell.

Most studies performed on non-B DNA sequences in oncogene promoter regions have focused on the G-quadruplex due to its inherent structural stability even at neutral pH. Indeed, G-quadruplex-forming sequences have been enormously investigated in terms of their folding topologies and the interactions between small molecules or DNA-binding proteins and G-quadruplex motifs.[9,18,19] In contrast, relatively few studies have been done on i-motif structures. The conformational change from the cytosine (C)-rich single-stranded DNA to i-motif takes place at slightly acidic pH (see Figure 1a).[20] The i-motif structure formed at slightly acidic pH consists of two parallel-stranded C:C+ hemiprotonated base-paired duplexes that are intercalated in an antiparallel manner, and its pH-dependent structure is significantly affected by the number of cytosine bases,[21] loop length,[22] environmental condition,[23−25] and attached or interacting material with the DNA strands.[26−28] It is known that C-rich sequences are present in or near the regulatory regions of >40% of all genes, including known oncogenes.[29] Recently, Rajendran et al. reported that i-motif structure can be formed by the molecular crowding even at neutral and slightly basic pH.[25] This being the case, an understanding on the mechanism and dynamics of the structural change of C-rich single-stranded

Received: July 4, 2011
Published: September 01, 2011

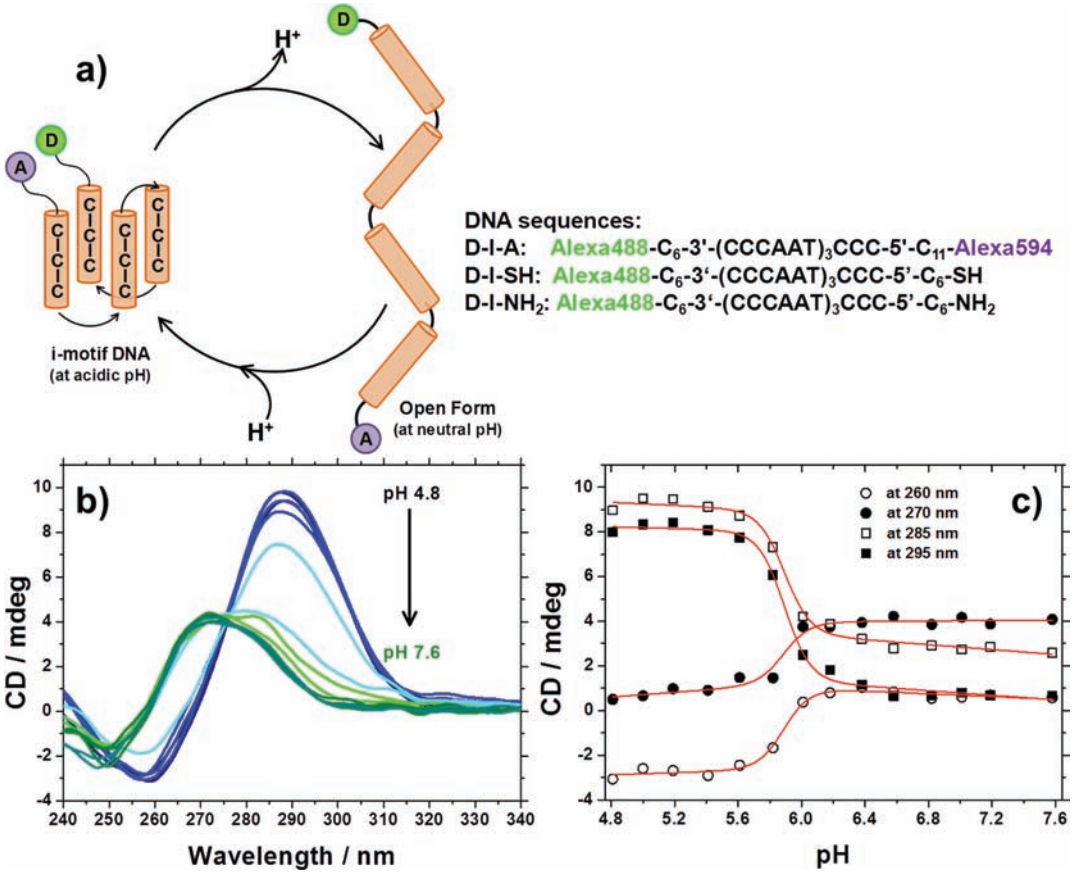

Figure 1. The pH-induced conformational change of i-motif and CD spectra. (a) Schematic illustration of the reversible pH-induced conformational change of i-motif and DNA sequences used in this study. (b) CD spectra of **D-I-A** in various pH solutions. The CD spectra were normalized at 350 nm. (c) Variation of CD intensity of **D-I-A** probed at different wavelength as a function of pH. Theoretical fits obtained from the fitting analysis are shown in red.

DNA is important. Nonetheless, its biological function and detailed conformation dynamics have not been clearly revealed yet.

In this work, we comprehensively investigated the mechanism and dynamics of the pH-induced structural change of i-motif using the combination of fluorescence resonance energy transfer (FRET) and fluorescence correlation spectroscopy (FCS) in the bulk phases and at the single-molecule level. Compared to the conventional techniques, such as circular dichroism (CD) and UV−vis spectroscopy, FRET and FCS methods are very useful tools to investigate the structure and the dynamics of a protein or DNA. FRET that is called as a molecular ruler is a unique technique to provide valuable information on the structure of biomolecules, such as a protein and DNA.[30] Furthermore, FCS is a very valuable tool to observe the translational diffusion of a biomolecule as well as the submicrosecond relaxation, such as the intrachain contact formation.[31,32] Using the FRET technique in the bulk phases and at the single-molecule level, we clearly show that the partially folded species as well as the single-stranded structure coexist at neutral pH. Furthermore, by measuring the FCS curves of i-motif, we clearly detected the gradual decrease of the diffusion coefficient (D) of i-motif with increasing pH, indicating the increase of the molecular size of i-motif. The quantitative analysis of FCS curves supports that the gradual decrease of D associated with the conformational change of i-motif is not only due to the change in the intermolecular interaction between i-motif and solvent accompanied by the increase of pH but also to the change of the shape of the DNA. In addition, i-motif, which has a compact tetraplex structure compared to the open form, shows a fast intrachain contact formation and dissociation due to the intrinsic conformational changes at the fluorescent site, including the motion of alkyl chain connecting the dye to DNA, whereas the open form shows a relatively slow intrachain contact reaction due to the DNA motion corresponding to an early stage interaction in the folding process of the unstructured open form. To our best knowledge, this is the first report for the fast event in the conformational dynamics of i-motif. We believe this will certainly contribute to the further understanding on in-depth biological studies of i-motif DNA and the range of its application.

2. EXPERIMENTAL SECTION

Full experimental details and characterization of compounds can be found in the Supporting Information. In order to prepare Alexa488-C_6-3′-$(CCCAAT)_3CCC$- 5′-C_{11}-Alexa594 (**D-I-A**), Alexa 594 was labeled to Alexa 488-labeled DNA sequence Alexa488-C_6-3′-$(CCCAAT)_3$-CCC-5′-C_6-SH (**D-I-SH**) obtained from Japan Bio Service. The obtained **D-I-A** was dissolved in various pH buffer solutions prepared by the alternate addition of 0.2 M of Na_2HPO_4 and 0.1 M of citric acid.[33]

The steady-state UV−vis absorption, fluorescence, and CD spectra were measured using a Shimadzu UV-3100, a Horiba FluoroMax-4, and JASCO CD-J720, respectively. The fluorescence lifetimes and FCS experiments of **D-I-A** and Alexa 488 with various pH solutions were

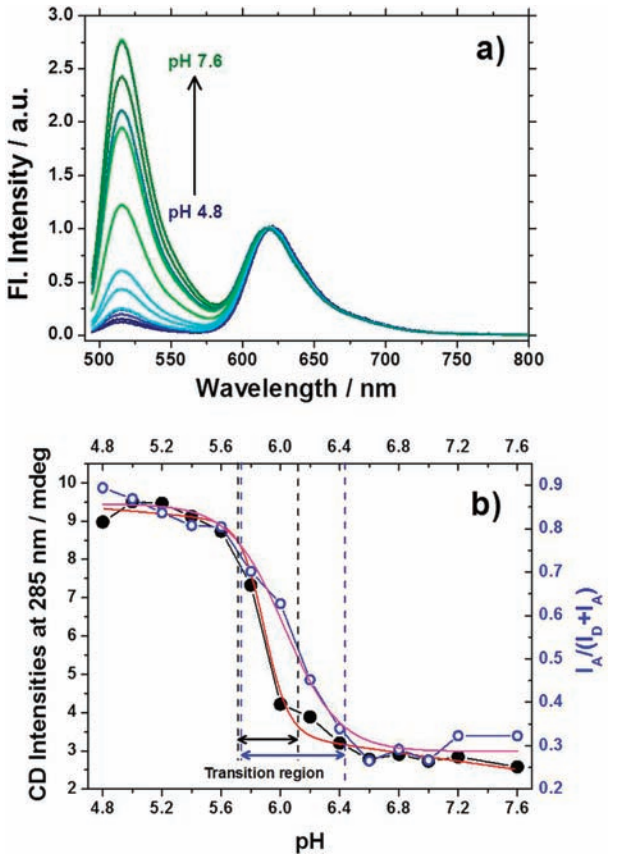

Figure 2. Fluorescence spectra and transition curve. (a) Fluorescence spectra of **D-I-A** in various pH solutions. The fluorescence spectra were normalized at 618 nm. (b) Changes in the ratio of the fluorescence intensities of acceptor to total emission ($I_A/(I_A + I_D)$) (○) and I_{CD} (●) of **D-I-A** probed at 285 nm, respectively, as a function of pH. Theoretical fits obtained from the fitting analysis are shown in red and pink for I_{CD} and ($I_A/(I_A + I_D)$), respectively.

measured with a time-resolved fluorescence microscope using confocal optics (MicroTime 200; PicoQuant, Berlin-Adlershof, Germany).

In order to measure the FRET efficiency of freely diffusing **D-I-A** at the single-molecule level, 1 nM of **D-I-A** solutions containing 1 mM of trolox and 10% β-mercaptoethanol by volume were prepared. Single-molecule FRET experiments were carried out with the same confocal optics (MicroTime 200; PicoQuant, Berlin-Adlershof, Germany) and two single photon avalanche photodiodes (Micro Photon Devices, PDM 50CT and 100CT) for the simultaneous detection of the FRET donor and acceptor. All samples were excited through an oil objective (Olympus, UPlanSApo, 1.40 NA, 100×) with a 485 nm pulsed laser (PicoQuant, full width at half-maximum 120 ps) controlled by a PDL-800B driver (PicoQuant). The excitation power of about 65 μW was used.

3. RESULTS AND DISCUSSIONS

In this study, we used 21-mer single-stranded DNA, of which both end-sides (5′ and 3′) were substituted by donor (Alexa 488) and acceptor (Alexa 594) dyes (Alexa 594-C_{11}-5′-CCC-(TAACCC)$_3$-3′-C_6-Alexa 488, **D-I-A**, see Figure 1a). First and foremost, we conducted the measurement of the melting temperature (T_m) to elucidate whether the DNA structure is affected by the covalent attachment of the dyes. The T_ms of **D-I-A** and **D-I-NH$_2$** in pH 4.8 buffer solutions are determined to be 55.8 ± 0.4 and 55.9 ± 0.4 °C, respectively (see Figure S1, Supporting Information). These T_m values are in accordance with that (T_m = 50.2 °C) of 5′-CCC(TAACCC)$_3$-3′ at pH 5.0 reported by Shin et al.[26] within an experimental error. These results indicate that the DNA structure remains almost intact after labeling with the dyes. Figure 1b shows CD spectra of **D-I-A** as a function of pH. Upon decreasing pH, the positive band near 270 nm and the negative band near 250 nm, which are due to base stacking and polynucleotide helicity of unstructured single-stranded DNA (open form),[34] respectively, are red-shifted to 285 and 260 nm with the increase of the ellipticity, respectively. These two distinct peaks at 285 and 260 nm are known as characteristic CD bands of i-motif structure.[25,35] This result means that the pH-induced conformational change goes from the open form to i-motif. As described in Figure 1c, the transition curves monitored by CD intensities show the sigmoidal feature, implying the conformational change of i-motif takes place via a two-state folding mechanism without any detectable intermediate. From the fitting results of the transition curves for **D-I-A**, the transition midpoint (x_0) is determined to be pH = 5.9.

On the other hand, the fluorescence intensities (I_f) of the donor (Alexa 488) attached to **D-I-A** is significantly quenched with decreasing pH (Figure 2a), whereas the fluorescence intensity of pristine Alexa 488 is independent in the range of pH 4−10 (see Figure S2, Supporting Information). Therefore, this suggests that the changes of the fluorescence intensities of **D-I-A** with decreasing pH are closely related to the conformational change of **D-I-A.** That is, upon decreasing pH, the open structure is folded to form i-motif with a tetrameric structure, resulting in the efficient FRET from donor (D) to acceptor (A). From the ratio of the fluorescence intensities of acceptor to total emission ($I_A/(I_A + I_D)$) of **D-I-A** as a function of pH, x_0 is determined to be pH = 6.0 (Figure 2b). Here, it is noteworthy that the value of x_0 is consistent with that determined from the CD intensity within an experimental error, while the transition region of the transition curve is wider than that obtained from the CD intensity (Figure 2b). This implies that the conformational change of i-motif could not be interpreted by simple two-state mechanism.

In order to further examine the conformational dynamics of **D-I-A** from open form (single-strand structure) to i-motif, we have measured the fluorescence lifetimes of **D-I-A** and **D-I-NH$_2$** as a function of pH. Figure 3a shows all fluorescence decay profiles of the donor dye (Alexa 488) of **D-I-A** measured in various pH solutions. All decay profiles measured from **D-I-NH$_2$** (and **D-I-SH**) can be fitted by a single exponential function with a relaxation time of 4.0 ± 0.1 ns (see Figures S3 and S4, Supporting Information). In contrast, all fluorescence decay profiles of donor of **D-I-A**, as shown in Figure 3a, were expressed by a biexponential function. By a simple analysis of all the fluorescence decay profiles, we found that at least three components with different fluorescence lifetimes are involved in the pH-induced conformational dynamics of **D-I-A**. Thus, we fitted all the decay profiles of **D-I-A** with a triexponential function. A global fitting analysis of all decay profiles revealed three relaxation times of 0.4, 1.0, and 2.8 ns in the pH-induced conformational change of **D-I-A**. As shown in Figure 3b, the fast component (τ_1 = 0.4 ns) is the major component at acidic solutions, whereas two components (τ_2 = 1.0 and τ_3 = 2.8 ns) with relatively slow decay times are dominantly observed at neutral pH solutions. Considering the conformational change between i-motif and the open form, two decay components should be observed in the time-resolved fluorescence experiments for the donor. However, as mentioned above, we could observe

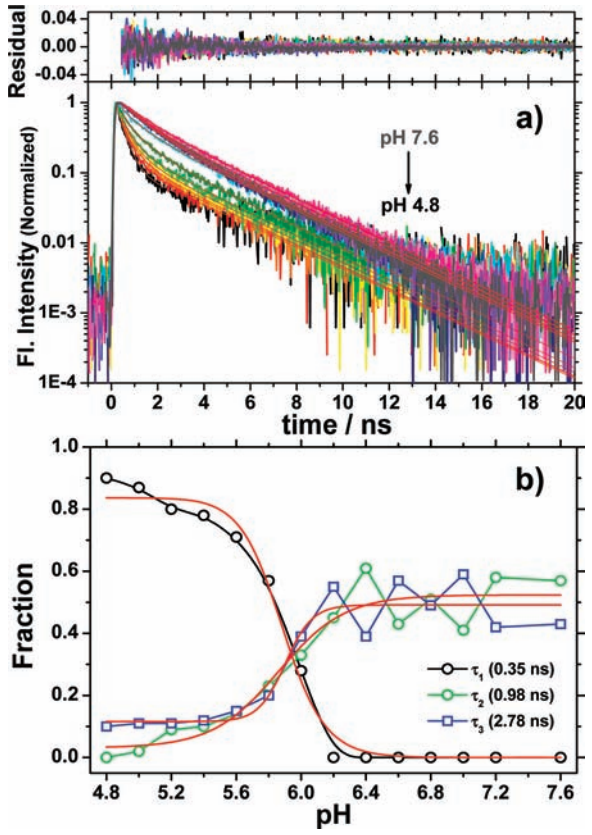

Figure 3. Fluorescence decay profiles and the fraction of the relevant decay components. (a) Global fitting results of fluorescence decay profiles of the donor attached to **D-I-A** as a function of pH. The theoretical fits obtained from the global fitting analysis are shown in red. (b) Changes in the fraction of the relevant decay components as a function of the pH.

three components with different fluorescence lifetimes from the pH-induced conformational change of i-motif, indicating that at least three species are involved in the pH-induced conformational change of i-motif. This result is in contrast with the result obtained by CD spectroscopy, showing the typical two-state transition. Recently, Trent groups reported that the CD spectra could not distinguish the different species with similar physical properties,[36] indicating that the CD signal is not a highly sensitive probe for the conformational change of DNA, such as G-quadruplex and i-motif. Interestingly, the decay times of two fast components ($\tau_1 = 0.4$ and $\tau_2 = 1.0$ ns) measured from donor in acidic and neutral pH solutions, respectively, were observed as the rise times in the acceptor's fluorescence decay profiles (see Figure S5, Supporting Information). These results indicate that although the structure of the fast-decay component of 0.4 ns observed at acidic pH is different from that at neutral pH, two fast components are attributable to a folded structure that can induce the fast energy transfer from the donor to the acceptor due to close proximity. Considering the pH-induced conformational change of i-motif, we suggest that the fast-decay component of 0.4 ns observed at acidic pH is attributed to i-motif, whereas the component of 1.0 ns may be attributed to a partially folded form, which can induce the energy transfer. Dhakal et al. found the coexistence of the partially folded form and i-motif in the C-rich human insulin linked polymorphism region (ILPR) oligonucleotides using the laser tweezers technique.[37] They also suggested that the formation of i-motif is decreased by increasing pH, while the partially folded structure with a small fraction is pH-independent (pH 5.5−7.0: 6.1%). Moreover, using experimental and theoretical methods, Dettler et al. reported that the classical i-motif structure is predominant at slightly acidic pH (pH 4.2−5.2), whereas i-motif-like is the most significant species at neutral pH.[38] These results agree with our results and support that the fast-decay component of 0.4 ns is attributed to i-motif, while 1.0 ns comes from the partially folded form. On the other hand, we suggest that although the fluorescence lifetime (2.8 ± 0.1 ns) of the slow-decay component observed from **D-I-A** is shorter than those (4.0 ± 0.1 and 3.9 ± 0.2 ns) of **D-I-NH$_2$** and **D-I-SH** (Figure S3 and S4, Supporting Information), the slow-decay component of 2.8 ns observed at neutral pH is attributed to the open form. The reason for the decrease of the fluorescence lifetime of donor molecule from 4.0 to 2.8 ns is probably due to a transient interaction between two dyes by the intrachain contact formation because there is no change in the fluorescence lifetime when DNA is singly labeled with a donor dye.

Generally, the FRET efficiency (E), which relates to the D's fluorescence lifetime, has been used as an indicator on D−A distance:[30]

$$E = 1 - \frac{\tau_{DA}}{\tau_D} = \left[1 + \left(\frac{r_{D-A}}{\mathbf{R}_0}\right)^6\right]^{-1} \quad (1)$$

where τ_{DA} and τ_D are the D's fluorescence lifetimes in the presence and absence of an acceptor, respectively, r_{D-A} is the D−A distance, and $\mathbf{R}_0$ is the Förster radius at which $E = 0.5$ ($\mathbf{R}_0$ for the Alexa 488 (D)−Alexa 594 (A) system is 60 Å;[39] $\tau_D = 4.0$ ns). Using fluorescence lifetimes determined at each pH, FRET efficiencies for i-motif and the partially folded form are calculated to be 0.90 and 0.75, respectively. Using eq 1, D−A distances (r_{D-A}) for i-motif and the partially folded form are calculated to be 4.2 and 5.0 nm, respectively. The r_{D-A} (4.2 nm) determined for i-motif is close to the maximum dimension of completely folded FDH (fullerene (C_{60}) attached to both end sides of 5′-CCC(TAACCC)$_3$-3′) reported by Shin et al (4.1 nm),[26] whereas the r_{D-A} (5.0 nm) for the partially folded form is greatly shorter than the maximum dimension of fully expanded FDH (7.8 nm), supporting that the fast-decay component of 1.0 ns has a partially folded form as explained above.

To confirm the coexistence of a partially folded form observed in the time-resolved fluorescence experiments, we have investigated the pH-induced conformation change of i-motif using single-molecule fluorescence spectroscopy. Single-molecule fluorescence spectroscopy provides an insight into the behavior of each individual molecule and consequently allows a detailed observation of subpopulations in structures or dynamics hidden under ensemble-averaged results.[40−42] Figure 4 displays the FRET efficiency distributions determined from the fluorescence intensity trajectories (FITs) of single-molecule **D-I-A** in solution at pH 4.8, 5.8, and 7.2. As depicted in Figure 4, the FRET histogram observed at pH 4.8 shows a single FRET peak centered at 0.86, whereas the FRET efficiency distributions of **D-I-A** at higher pH (pH 5.8 and 7.2) show three distinct peaks (0.32, 0.59, and 0.86; the peak with $E_{FRET} \sim 0.05$ is probably attributed to the DNA singly labeled with a donor dye). Interestingly, the peak at $E_{FRET} \sim 0.86$ observed at pH 4.8 is close to that ($E_{FRET} \sim 0.90$) observed from the fluorescence lifetimes of i-motif form within an experimental error. In addition, with increasing the pH, the

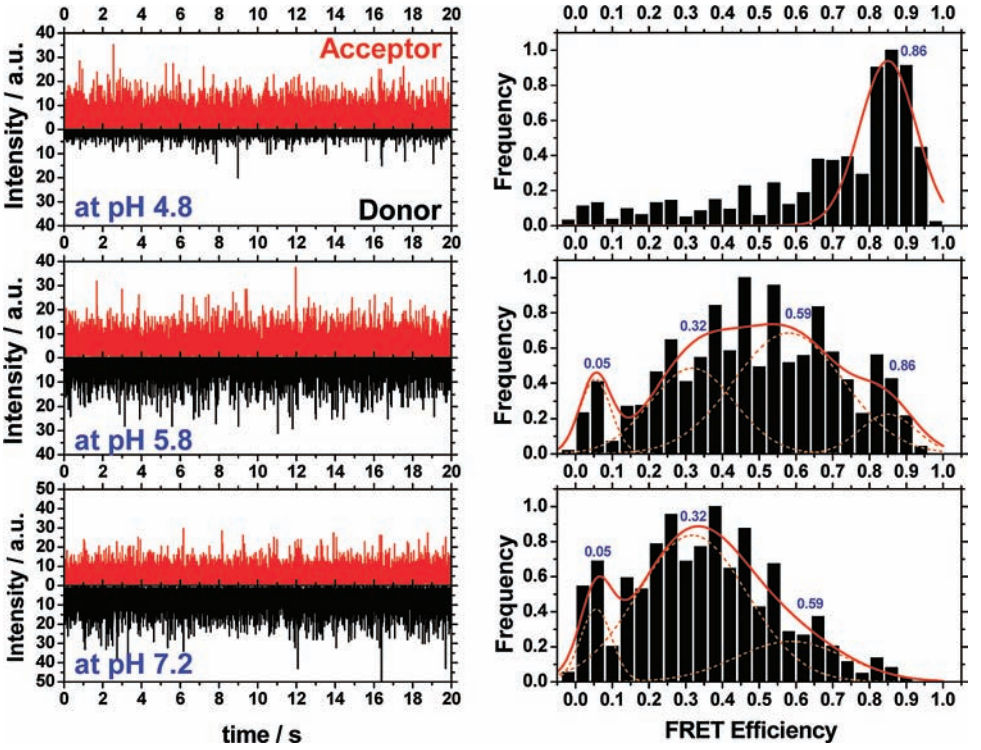

Figure 4. Single-molecule Spectroscopy. FITs (a, c, and e) and FRET efficiency distributions (b, d, and f) of single-molecule **D-I-A** at pH 4.8 (top), 5.8 (middle), and 7.2 (bottom) (binning time: 1 ms). The red solid lines denote the Gaussian fitting curves. The peak with $E_{FRET} \sim 0.05$ is probably attributed to the DNA which is singly labeled with a donor dye.

population of the component with $E_{FRET} \sim 0.86$ is disappeared, and then the peaks at E_{FRET} ~0.32 and ~0.59 are observed as main components at a higher pH. Considering the pH-induced conformational change of i-motif, we suggest that the component with E_{FRET} ~0.86 is attributed to i-motif. On the other hand, using eq 1, the r_{D-A}s for the structural species with $E_{FRET} \sim 0.32$ and 0.59 are calculated to be 6.8 and 5.6 nm, respectively. These values are close to those of fully expanded FDH (7.8 nm)[26] and the partially folded form (5.0 nm) observed in the time-resolved fluorescence experiment within an experimental error, indicating that two low FRET efficiencies of 0.32 and 0.59 come from the open form and the partially folded form, respectively. These results support that the partially folded species, which could not be observed by the CD spectra, coexist with the single-stranded structure at neutral pH. Here, it is noteworthy that the partially folded form reported in this study is not observed at acidic pH, whereas that proposed by Dhakal et al. is pH independent (pH 5.5−7.0: 6.1%).[37] This means that each partially folded form proposed by this study and by Dhakal et al. may have a different structure.

In addition, although i-motif forming sequences are considered to be present in the promoter regions of various well-known oncogenes[5] and telomeric DNA,[6] the structure of i-motif in vivo has not been directly observed. One of the reasons might be the neutral environment of cellular interior, whereas i-motif is dominantly formed by hemiprotonation of cytosine base at acidic condition. However, as mentioned previously, C-rich single-stranded DNA can form i-motif structures not only at acidic pH but also at neutral and slightly basic pH under molecular crowding condition, which is similar to the intracellular environment.[25] Considering those previous studies, therefore, the formation of i-motif in vivo is theoretically possible. Thus, it is extremely crucial to confirm the existence of i-motif (or the partially folded form and i-motif-like form) at neutral pH. In this respect, the result presented here implies that the partially folded species may exist substantially in vivo and play an important role in a biological function, such as replication, regulation, and transcription in physiological conditions.

In order to further elucidate the conformational dynamics of i-motif, we measured the molecular diffusion time of **D-I-A** at various pHs. The molecular diffusion time certainly reflects not only the global structural change of a biomolecule occurring in a protein or DNA folding/unfolding process but also the intermolecular interaction between a biomolecule and solvent molecules.[43−45] Thus, the molecular diffusion time can directly provide the information on the change in molecular size associated with the conformational change of a biomolecule. In this respect, FCS is a very useful tool to observe the translational diffusion of a biomolecule as well as the submicrosecond relaxation corresponding to the intrachain contact formation.[31,32,46] To elucidate the translational diffusion of i-motif, we measured the FCS curve of **D-I-A** at various pHs. In the presence of a dynamic process, such as conformational relaxation resulting in a change of the fluorescence intensity, the autocorrelation function can be expressed by

$$G(\tau) = \frac{1}{N}\left(1 + \frac{\tau}{\tau_{diff}}\right)^{-1}\left[1 + K^{c}_{obsd}\exp\left(\frac{\tau}{\tau^{c}_{obsd}}\right)\right] \quad (2)$$

where N is the average number of molecules in the observed volume, τ_{diff} is the molecular diffusion time, K^{c}_{obsd} is the observed amplitude of the intrachain contact formation kinetics due to changes of the donor−acceptor distance, and τ^{c}_{obsd} is the observed

dx.doi.org/10.1021/ja2061984 |J. Am. Chem. Soc. 2011, 133, 16146–16153

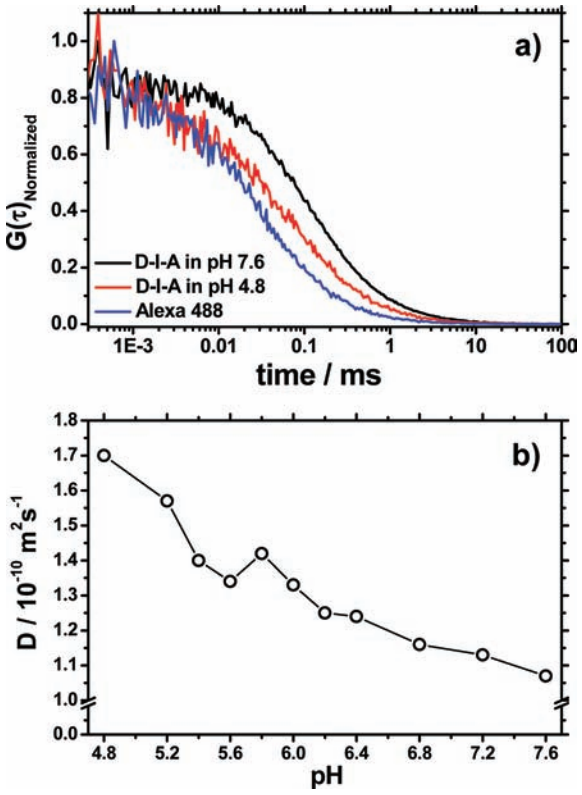

Figure 5. Representative FCS curves and the variation of the diffusion coefficient. (a) Representative FCS data of Alexa 488 at pH 7.0 and **D-I-A** at pH 4.8 and 7.6. (b) Plot of the variation of the molecular diffusion coefficients (D) of **D-I-A** determined in various pH solutions.

time of intrachain contact formation. Figure 5a shows the representative FCS data of Alexa 488 at pH of 7.0 and **D-I-A** recorded at pH 7.6 and 4.8 (see also Figure S6, Supporting Information). From the molecular diffusion times obtained by the FCS analysis using eq 2 and the diffusion coefficient ($D = 4.5 \times 10^{-10}$ m^2 s^{-1}) of Alexa 488 at neutral pH,[47] we found that the diffusion coefficient of **D-I-A** gradually decreased upon increasing pH (Figure 5b). Since the diffusion coefficient is inversely proportional to the hydrodynamic radius (R_h) of a molecule, the decrease of Ds with increasing pH indicates that the hydrodynamic radius of the open form is 1.6 times larger than that of i-motif ($R_{h\_open}/R_{h\_i\text{-}motif} \cong 1.6$). In addition, it is notable that the molecular size of i-motif is gradually increasing with pH.

There are several factors that govern the diffusion process of molecules in solution; that is, the size, shape of the molecule, and intermolecular interaction between the solvent and the diffusing molecule. To investigate the origin of the slow diffusion of the open form, we examine the effect of the molecular shape on D. According to the Stokes equation, the frictional coefficient (f_0) for a spherical molecule is expressed as follows:[48]

$$f_0 = 6\pi\eta R_0 \tag{3}$$

where η is the viscosity of the solvent, and R_0 is the radius of a spherical molecule. Generally, the frictional coefficient (f) of the molecule in solution depends on its size and shape. When the shape is deformed from the spherical symmetry, the friction should be different from eq 3. Although we do not know the exact shape of the partially folded and the open form, some previous studies have suggested that the partially folded form has a triplex structure, which is similar to the tetraplex structure of i-motif.[33,45] Thus, we can assume that i-motif and the partially folded form have a spherical shape. In contrast, it is reasonable enough to assume that the open form has a rod-like shape because duplex DNA generally behaves like a rigid rod, and **D-I-A** consists of the short 21-mer DNA sequence, which has a helical structure.[26,49] If the molecule possesses a rod-like shape, f/f_0 is given by[48]

$$\frac{f}{f_0} = \frac{(2/3)^{1/3}(a/b)^{2/3}}{\ln 2(a/b) - 0.3} \tag{4}$$

where a is the half-length, and b is the radius. The a and b in the case of a single-stranded **D-I-A** are calculated to be roughly 3.8 and 0.3 nm, respectively. Using eq 4, f/f_0 value of the single-stranded **D-I-A** is calculated to be 1.62, which is close to the experimentally observed value ($R_{h\_open}/R_{h\_i\text{-}motif} \cong f/f_0 \cong 1.6$). This agreement indicates that the change of the shape of i-motif plays an important role in its diffusion process. However, the shape of the open form at neutral pH should be near to a random coil rather than a rigid rod because of its high flexibility to access various conformations. Furthermore, the gradual decrease of D associated with the conformational change of i-motif cannot be explained only by the effect of the molecular shape on D. As mentioned above, the molecular diffusion process is greatly affected by the intermolecular interaction between a biomolecule and solvent molecules. At neutral pH, the single-stranded DNA has a random coil structure, and consequently its solvent-exposed surface area increases, indicating the increase in the binding site of water upon a DNA. Hence the solvent molecules will easily interact with DNA, and consequently the DNA molecule feels more frictional drag in the solvent, and its diffusion is more restrained than in the case of i-motif and partially folded form. Practically, the conformational change of i-motif is substantially initiated by the deprotonation of cytosine in two parallel-stranded C:C+ base-paired duplex, leading to the increase of the interaction between the i-motif and water molecules. Thus, DNA molecule at neutral pH is subjected to a more frictional constraint in the solvents than at an acidic pH. It is well-known that the stability of G-quadruplex structure and the B-form in duplex DNA are regulated by hydration;[24,50,51] for instance, the thermodynamic stability of G-quadruplex increases as the water activity is reduced (dehydration), and the surface area accessible to water is minimized. In addition, Sherman et al. showed that the denaturant-induced unfolding reaction of protein L leads to the gradual expansion of the radius of gyration due to the interaction between solvent molecules and a protein, and the solvation energy associated with the denaturation of a protein is linearly increased.[52] These results indicate that the hydration has a vital role in the stabilization of DNA (or protein). From this point of view, the gradual decrease of D associated with the conformational change of i-motif is not only due to the continuous change in the intermolecular interaction between i-motif and solvent accompanied by the increase of pH but also to the change in its shape.

Additionally, we could observe the partially folded form at neutral pH using time-resolved fluorescence and single-molecule spectroscopy. Recently, Dhakal et al. and Dettler et al. found the coexistence of the partially folded form and i-motif at neutral pH.[37,38] Furthermore, it has been suggested that C-rich DNA can form multiple i-motif structures.[53,54] In light of the previous reports and our results, we cannot exclude the possibility that the

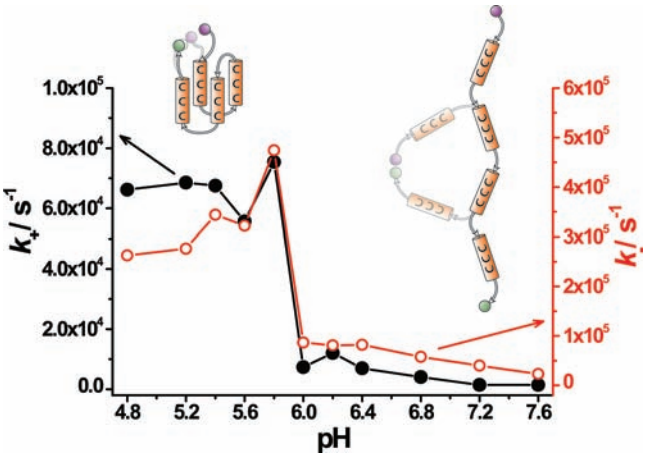

Figure 6. Rates of the intrachain contact formation (k_+, filled circle) and dissociation (k_-, open circle) of **D-I-A** determined from the FCS experiments as a function of pH. Responsive fluctuational motions occurred at i-motif and open form are illustrated representatively in left and right sides, respectively.

gradual change in the molecular size shown in Figure 5b is due to the existence of spectrally silent multiple species.

On the other hand, FCS can observe the submicrosecond relaxation corresponding to intrachain contact formation or fast folding events of a biomolecule as mentioned previously.[31,32,46] Since the intrachain contact formation is recognized as an early stage interaction in the folding process of a biomolecule, an elucidation of the intrachain contact formation is important for understanding the mechanism and dynamics of the conformational change of i-motif. Figure 6 shows the rate constants of intrachain contact formation calculated from the observed amplitude and the observed time constant (see Supporting Information). As given in Figure 6, rate constants of the intrachain contact formation (k_+) and dissociation (k_-) show the sigmoidal feature. The averaged $\langle k_+ \rangle$ of **D-I-A** at acidic and neutral pH is determined to be $(6.7 \pm 0.7) \times 10^4\ s^{-1}$ and $(5.5 \pm 4.1) \times 10^3\ s^{-1}$, respectively, whereas the averaged $\langle k_- \rangle$ was calculated to be $(3.4 \pm 0.8) \times 10^5$ and $(6.2 \pm 2.6) \times 10^4\ s^{-1}$, respectively. Considering the main species of each pH, the $\langle k_+ \rangle$ and $\langle k_- \rangle$ observed at acidic and neutral pH may correspond to rate constants of end-to-end contact formation and dissociation of i-motif and the open form, respectively. Especially, the $\langle k_+ \rangle$ and $\langle k_- \rangle$ observed at neutral pH are close to those for 21-mer DNA hairpin, $(dT)_{21}$ and $(dA)_{21}$, reported by Bonnet et al.[32] within an experimental error, supporting the rates observed in this study are due to the intrachain contact formation and dissociation of DNA. Here, it is noteworthy that the k_+ and k_- for i-motif are 5−10 times faster than those for the open form. Although i-motif has a compact tetraplex structure compared to the open structure, there are intrinsic conformational changes at the fluorescent site, including the motion of the alkyl chain connecting the labeled dye to DNA. These fluctuational movements, such as the intrachain contact formation and dissociation, bring about a change of the fluorescence intensity. In contrast, as explained previously, the open structure is subjected to a more frictional constraint in the solvents than i-motif because of the increased hydration and its restrained dynamic flexibility. Conversely, the dynamic flexibility of i-motif at acidic pH is increased by the dehydration. Moreover, the distance between two dyes in the open form is farther than in i-motif structure. Accordingly, the intrachain contact formation for the open form should be much slower compared to that for i-motif. In addition, the slow intrachain contact formation observed from the open form may be attributed to an early stage interaction in the folding process of the unstructured open form. Since most of the studies for the intrachain contact formation of DNAs have been carried out with unstructured DNAs, there was no observation for the structured DNA, such as i-motif. To our best knowledge, this is the first report for the intrachain contact formation of i-motif.

4. CONCLUSIONS

We thoroughly investigated the pH-induced conformational dynamics of i-motif using the combination of FRET and FCS techniques. It is known that i-motif can be formed at not only acidic pH but also at neutral pH under molecular crowding conditions, which is similar to the intracellular environment.[25] In addition, C-rich sequences are known to be present in or near the regulatory regions of >40% of all genes (including known oncogenes).[29] In light of those previous studies, the formation of i-motif in vivo is theoretically possible, and an understanding on the mechanism and dynamics of the structural change of C-rich single-stranded DNA is extremely important. In addition, despite numerous studies on i-motif, its detailed conformational dynamics have been rarely reported. Using the FRET technique in the bulk phases and at the single-molecule level, we clearly show that the partially folded species, which could not be observed by the CD spectra, coexist with the single-stranded structure at neutral pH, supporting that the partially folded species may exist substantially in vivo and play an important role in a process of gene expression. Furthermore, we clearly observed the dynamics due to the intrachain contact formation and dissociation as well as the changes of the diffusion coefficient of i-motif with increasing pH. From the quantitative analysis of FCS curves, we found that the gradual decrease of the diffusion coefficient (D) of i-motif with increasing pH can be interpreted in terms of the continuous change in the intermolecular interaction between i-motif and solvent accompanied by the increase of pH and the change of the shape of the DNA. Moreover, FCS analysis showed that the intrachain contact formation and dissociation for i-motif are 5−10 times faster than that for the open form. The fast dynamics of i-motif with a compact tetraplex is due to the intrinsic conformational changes at the fluorescent site, including the motion of alkyl chain connecting the dye to DNA, whereas the slow intrachain contact formation observed from the open form is due to the DNA motion, corresponding to an early stage interaction in the folding process of the unstructured open form. We believe this will certainly contribute to further progress on in-depth biological studies of i-motif DNA and the range of its application. In future work, we intend to study the conformational change of i-motif in a living cell.

■ ASSOCIATED CONTENT

Supporting Information. Detailed information on the experimental procedures and data analysis of single-molecule FRET and FCS experiments. Additional figures about T_m measurements (Figure S1), fluorescence decay profiles of **D-I-NH$_2$**, **D-I-SH** and single dyes (Figures S2−S5), and FCS measurements (Figures S6−S8). This material is available free of charge via the Internet at http://pubs.acs.org.

AUTHOR INFORMATION

Corresponding Author
majima@sanken.osaka−u.ac.jp

ACKNOWLEDGMENT

T.M. thanks to the World Class University (WCU) program through the National Research Foundation of Korea funded by the Ministry of Education, Science, and Technology (R31-10035) for the support. This work has been partly supported by a Grant-in-Aid for Scientific Research (projects 22245022 and others) from the Ministry of Education, Culture, Sports, Science, and Technology (MEXT) of Japanese Government.

REFERENCES

(1) Bacolla, A.; Wells, R. D. *Mol. Carcinog.* **2009**, *48*, 273.
(2) Wang, G.; Vasquez, K. M. *Mutat. Res.* **2006**, *598*, 103.
(3) Phan, A. T.; Kuryavyi, V.; Patel, D. J. *Curr. Opin. Struct. Biol.* **2006**, *16*, 288.
(4) Rankin, S.; Reszka, A. P.; Huppert, J.; Zloh, M.; Parkinson, G. N.; Todd, A. K.; Ladame, S.; Balasubramanian, S.; Neidle, S. *J. Am. Chem. Soc.* **2005**, *127*, 10584.
(5) Brooks, T. A.; Kendrick, S.; Hurley, L. *FEBS J.* **2010**, *277*, 3459.
(6) Phan, A. T.; Mergny, J. L. *Nucleic Acids Res.* **2002**, *30*, 4618.
(7) Ahmed, S.; Kintanar, A.; Henderson, E. *Nat. Struct. Biol.* **1994**, *1*, 83.
(8) Brooks, T. A.; Hurley, L. H. *Nat. Rev. Cancer* **2009**, *9*, 849.
(9) Wu, Y.; Brosh, R. M., Jr. *FEBS J.* **2010**, *277*, 3470.
(10) Balasubramanian, S.; Neidle, S. *Curr. Opin. Chem. Biol.* **2009**, *13*, 345.
(11) Xu, Y.; Hirao, Y.; Nishimura, Y.; Sugiyama, H. *Bioorg. Med. Chem.* **2007**, *15*, 1275.
(12) Wang, C.; Huang, Z.; Lin, Y.; Ren, J.; Qu, X. *Adv. Mater.* **2010**, *22*, 2792.
(13) Yang, Y.; Liu, G.; Liu, H.; Li, D.; Fan, C.; Liu, D. *Nano Lett.* **2010**, *10*, 1393.
(14) Modi, S.; M, G. S.; Goswami, D.; Gupta, G. D.; Mayor, S.; Krishnan, Y. *Nat. Nanotechnol.* **2009**, *4*, 325.
(15) Krishnan, Y.; Simmel, F. C. *Angew Chem. Int. Ed.* **2011**, *50*, 3124.
(16) Shieh, Y. A.; Yang, S. J.; Wei, M. F.; Shieh, M. J. *ACS Nano* **2010**, *4*, 1433.
(17) Neidle, S. *Curr. Opin. Struct. Biol.* **2009**, *19*, 239.
(18) Huppert, J. L. *FEBS J.* **2010**, *277*, 3452.
(19) Bardin, C.; Leroy, J. L. *Nucleic Acids Res.* **2008**, *36*, 477.
(20) Gehring, K.; Leroy, J. L.; Gueron, M. *Nature* **1993**, *363*, 561.
(21) Mergny, J.-L.; Lacroix, L.; Han, X.; Leroy, J.-L.; Helene, C. *J. Am. Chem. Soc.* **1995**, *117*, 8887.
(22) Kendrick, S.; Akiyama, Y.; Hecht, S. M.; Hurley, L. H. *J. Am. Chem. Soc.* **2009**, *131*, 17667.
(23) Zhou, J.; Wei, C.; Jia, G.; Wang, X.; Feng, Z.; Li, C. *Mol. Biosyst.* **2010**, *6*, 580.
(24) Miyoshi, D.; Karimata, H.; Sugimoto, N. *J. Am. Chem. Soc.* **2006**, *128*, 7957.
(25) Rajendran, A.; Nakano, S.; Sugimoto, N. *Chem. Commun.* **2010**, *46*, 1299.
(26) Shin, S. R.; Jin, K. S.; Lee, C. K.; Kim, S. I.; Spinks, G. M.; So, I.; Jeon, J.-H.; Kang, T. M.; Mun, J. Y.; Han, S.-S.; Ree, M.; Kim, S. J. *Adv. Mater.* **2009**, *21*, 1907.
(27) Li, X.; Peng, Y.; Ren, J.; Qu, X. *Proc. Natl. Acad. Sci. U.S.A.* **2006**, *103*, 19658.
(28) Fedoroff, O. Y.; Rangan, A.; Chemeris, V. V.; Hurley, L. H. *Biochemistry* **2000**, *39*, 15083.
(29) Huppert, J. L.; Balasubramanian, S. *Nucleic Acids Res.* **2007**, *35*, 406.
(30) Lakowicz, J. R. *Principles of fluorescence spectroscopy*; 3rd ed.; Springer: New York, 2006.
(31) Choi, J.; Kim, S.; Tachikawa, T.; Fujitsuka, M.; Majima, T. *Phys. Chem. Chem. Phys.* **2011**, *13*, 5651.
(32) Bonnet, G.; Krichevsky, O.; Libchaber, A. *Proc. Natl. Acad. Sci. U.S.A.* **1998**, *95*, 8602.
(33) McIlvaine, T. C. *J. Biol. Chem.* **1921**, *49*, 183.
(34) Rajendran, A.; Nair, B. U. *Biochim. Biophys. Acta* **2006**, *1760*, 1794.
(35) Guo, K.; Gokhale, V.; Hurley, L. H.; Sun, D. *Nucleic Acids Res.* **2008**, *36*, 4598.
(36) Dailey, M. M.; Miller, M. C.; Bates, P. J.; Lane, A. N.; Trent, J. O. *Nucleic Acids Res.* **2010**, *38*, 4877.
(37) Dhakal, S.; Schonhoft, J. D.; Koirala, D.; Yu, Z.; Basu, S.; Mao, H. *J. Am. Chem. Soc.* **2010**, *132*, 8991.
(38) Dettler, J. M.; Buscaglia, R.; Cui, J.; Cashman, D.; Blynn, M.; Lewis, E. A. *Biophys. J.* **2010**, *99*, 561.
(39) Rothwell, P. J.; Mitaksov, V.; Waksman, G. *Mol. Cell.* **2005**, *19*, 345.
(40) Roy, R.; Hohng, S.; Ha, T. *Nat. Methods* **2008**, *5*, 507.
(41) Liu, R.; Hu, D.; Tan, X.; Lu, H. P. *J. Am. Chem. Soc.* **2006**, *128*, 10034.
(42) Tan, X.; Nalbant, P.; Toutchkine, A.; Hu, D. H.; Vorpagel, E. R.; Hahn, K. M.; Lu, H. P. *J. Phys. Chem. B* **2004**, *108*, 737.
(43) Terazima, M. *Phys. Chem. Chem. Phys.* **2006**, *8*, 545.
(44) Choi, J.; Terazima, M. *J. Phys. Chem. B* **2002**, *106*, 6587.
(45) Choi, J.; Yang, C.; Kim, J.; Ihee, H. *J. Phys. Chem. B* **2011**, *115*, 3127.
(46) Neuweiler, H.; Johnson, C. M.; Fersht, A. R. *Proc. Natl. Acad. Sci. U.S.A.* **2009**, *106*, 18569.
(47) Nitsche, J. M.; Chang, H. C.; Weber, P. A.; Nicholson, B. J. *Biophys. J.* **2004**, *86*, 2058.
(48) Van Holde, K. E.; Johnson, W. C.; Ho, P. S. *Principles of physical biochemistry*; 2nd ed.; Pearson/Prentice Hall: Upper Saddle River, N.J., 2006.
(49) Jin, K. S.; Shin, S. R.; Ahn, B.; Rho, Y.; Kim, S. J.; Ree, M. *J. Phys. Chem. B* **2009**, *113*, 1852.
(50) Miller, M. C.; Buscaglia, R.; Chaires, J. B.; Lane, A. N.; Trent, J. O. *J. Am. Chem. Soc.* **2010**, *132*, 17105.
(51) Miyoshi, D.; Nakamura, K.; Tateishi-Karimata, H.; Ohmichi, T.; Sugimoto, N. *J. Am. Chem. Soc.* **2009**, *131*, 3522.
(52) Sherman, E.; Haran, G. *Proc. Natl. Acad. Sci. U.S.A.* **2006**, *103*, 11539.
(53) Dai, J.; Hatzakis, E.; Hurley, L. H.; Yang, D. *PLoS One* **2010**, *5*, e11647.
(54) Dai, J.; Ambrus, A.; Hurley, L. H.; Yang, D. *J. Am. Chem. Soc.* **2009**, *131*, 6102.